Desalination and Water Treatment
www.deswater.com
20 (2010) 313–323
August
1944-3994 / 1944-3986 © 2010 Desalination Publications. All rights reserved.
doi: 10.5004/dwt.2010.1350

Investigation studies of vapor side corrosion in a multistage flash desalination pilot plant

A. Al-Arifi[a]*, I.S. Al-Mutaz[b], M.A. Alodan[b], F. Abudaleem[b]

[a]*Saline Water Conversion Corporation, P.O. Box 5968, Riyadh 11432, Saudi Arabia*
Tel. +966 (1) 4665030; Fax +966 (1) 4644179; email: aalarifi@swcc.gov.sa
[b]*Departement of Chemical Engineering, King Saud University, P.O. Box 800, Riyadh 11421, Saudi Arabia*

Received 1 May 2009: Accepted in revised form 4 April 2010

ABSTRACT

Vapor side corrosion (VSC) is one among different forms of corrosion encountered in multistage flash desalination (MSF). Vapor side corrosion is generally provoked and enhanced due to the presence of CO_2, O_2 and other non-condensable gases. Vapor side corrosion exhibits a major problem in both acid as well as additive dosed MSF plants. Although VSC has been reported by many workers in desalination field, only few studies were carried out in laboratory simulating real plant environment. The impact of vapor side environment on the corrosion rate of two commonly used materials of construction Cu-Ni 70/30 and Cu-Ni 90/10 was investigated at three levels of study through research program at an MSF actual plant, MSF pilot plant and in bench scale experimental up. This paper reports the studies carried out at an MSF pilot plant with capacity 20 m^3/d located at SWCC Al Jubail (SWDRI) by exposing Cu-Ni 70/30 and Cu-Ni 90/10 at four different top brine temperatures employed usually in MSF plants (90°C, 100°C,110°C and 119°C). The coupons exposed for 20 days in stage one, three and stage five in vertical and horizontal positions. Each stage has different temperature at brine and vapor sides. Experiments were carried out using actual chlorinated seawater from the Arabian Gulf. The results indicate that 70/30 Cu-Ni is more corrosion resistant than 90/10 Cu-Ni alloys. The corrosion rate for the coupons in horizontal position is higher than in vertical position tests. There is no clear effect of top brine temperature on the corrosion rate of copper nickel alloys. The corrosion rate at 90°C is higher than at 119°C which indicates that the air leakage is a strong factor and also the corrosion rate in stage three is more than in another stage in some tests. Different techniques employed in these studies include weight loss measurement, SEM and EDX.

Keywords: Multistage flash desalination; Non-condensable gases; Condenser tube vapor; Stage

1. Introduction

Heat exchanger tube is the most costly item in the multistage flash desalination (MSF) process. Heat exchanger tubes in MSF plants face severe corrosion due to their exposure to very fast hot dearated brine inside the tube and condensing vapor on its outside surface. The corrosion problem at the vapor side is generally provoked due to uncertainties in concentrations of non-condensable gases (NCG) such as CO_2, O_2 and others. Vapor side corrosion (VSC) is a major problem in both acid and additive dosed MSF plants due to the high corrosive environments inside

* Corresponding author.

the flash chamber. In vapor space zone the environments consist in addition to the gases evolved during evaporation or air leakage to the unit due to reduced pressure, high vapor velocity released which has varying velocities depending on the pressure in the unit and design.

Occurrence of leakage of copper–nickel heat transfer tubes due to VSC problem occurred in a number of plants in different countries. It happened mostly in MSF plants but pt also occurred in MED plants. VSC indicates that corrosion starts from the vapor side possibly leading to the thinning of tube walls until they yield to pressure of water side. It also affects the inter-stage wall, support plate and venting system components [1]. VSC of condenser tubes is basically electrochemical in nature, it involves reduction of oxygen gas in the vapor and building up the copper oxide on the tube surface. This type of corrosion can be recognized through an above normal Cu^{2+} content of distillate water and an increase in distillate conductivity. The main factors affecting VSC is operation problems and venting system design. Mal operation due to inadequate deaerator capacity results in the increase of the dissolved oxygen in the recirculated brine. While if the venting system design is not completely effective, there is a chance of accumulation of NCG inside the flash unit, therefore, the corrosion mechanism and rate in the vapor side is strongly related to the performance of the ventilation system. The life of MSF plant is likely to be decided by VSC [2].

The tube failure occurs due to the presence of pockets of CO_2 gas near the tube, which re-dissolve in distillate to form an aggressive solution. Some of CO_2 is transferred down the plants via the product water transfer duct. The tube failure usually occurs in the high temperature stage and the middle stage due the accumulation of NCG and after years of operation shorter than projected plant life time of the plant, pitting, tube thinning, galvanic etc. forms of VSC were reported [2]. Fig. 1 shows photographs from some of Saline Water Conversion Corporation (SWCC) plants which were prone to VSC. These photographs show the severity of VSC. Cases of VSC are less well studied compared to water side. Understanding of VSC mechanism is complicated by the possibility of the presence of transition physical and chemical environment conditions. Possible aggressive pollutants which may be present on the transient basis are chlorine, bromine, hydrogen sulfide and ammonia. In the units where VSC has been reported, it appears to be most in the lower part of the cold end tube sheet. The film running down inside the cold end tube sheet apparently allows enough sub-cooling for the pH to drop sufficiently for corrosion to start if oxygen is present. As the film runs down the inside of the tube sheet, the driving force to vent the NCG decrease allowing a "bubble of NCG" to form and persist in the lower part of the tube bundle at the cold end tube sheet [3].

In acid dosed MSF plants, almost all the CO_2 is removed by the decarobonator; CO_2 is present along with O_2 as NCG in additive treatment plants. Other gases such as H_2S, NH_3, Br_2 and Cl_2 may be also present in significant concentration and could be responsible for corrosion attacks [4,5]. Most studies related to VSC can be divided into theoretical, experimental and practical (plant experience) studies. Comprehensive review on vapor side corrosion has been reported [6–8]. The review indicated the availability of scanty of literature and there are few studies carried out on the problems of VSC, and in most of the reported literature real plant conditions were not simulated in laboratory studies and hence the clear mechanism of VSC is not fully understood. Most of the experimental studies with the aim to simulate VSC, such as studies by Shams El Din [9], Hodgkiess [10], Al Subaie [11], Al Thubaiti [12] were done by using distillate water (water vapor) and injecting CO_2/O_2 for a short period of time at ambient temperature to 80°C or using solution with different chloride [13]. Recent studies by El-Sayed [14] with a test unit imitate both the liquid and vapor environments. These experiments in general did not simulate real MSF plants conditions

A research project to study the corrosion behavior of the commercially available copper nickel alloys used in heat exchanger tubes utilized in desalination plants was carried out. Different experiments were designed and carried out in different environments ranging from real exposure of the coupon in actual working plants for more than one year in one of SWCC commercial plants (Al-Shoiba Desalination Plant phase I), MSF pilot plant

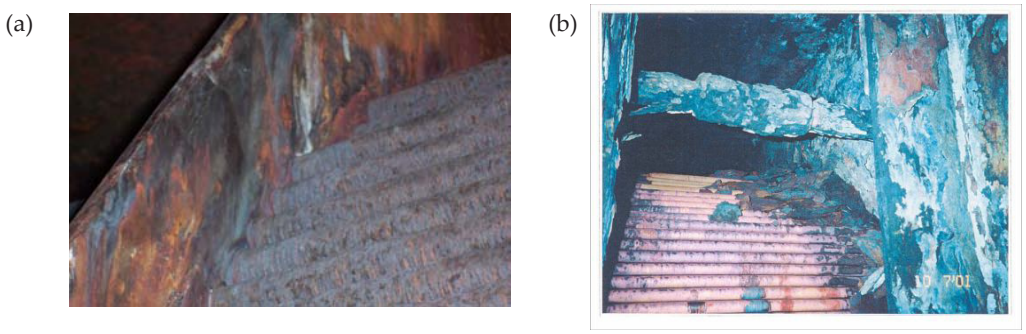

Fig. 1. VSC in MSF plant: (a) Non-lining area above the demister of the partition plate; (b) Vapor side corrosion of Cu-Ni tubes.

at SWDRI-Al-Jubail and studies in a bench scale experimental setup with different concentrations of NCG. These experimental studies aim to find the role played by NCG in vapor side corrosion.

In this paper the findings of the studies carried out at the MSF pilot plant are presented for copper nickel tubes (70/30 and 90/10).

2. Experimental methodology in MSF pilot plant

Different experiments were carried out in an MSF pilot plant in Saline Water Desalination Research institute (SWDRI) belonging to SWCC at Al-Jubail. The MSF pilot plant capacity is 20 m^3/d and it consists of total six stages with four stages in the heat recovery section and two stages in the heat rejection section. The MSF pilot plant has all important features of a fully established MSF commercial plant in design and performance. The make-up seawater can be given additive and/or acid treatment inclusive of external deaerator and decarbonator. There is also a provision for acid cleaning of heat transfer tubes. Fig. 2 shows a photograph of the MSF pilot plants in SWDRI and Fig. 3 shows a schematic diagram. of the MSF plant.

Fig. 2. MSF pilot plant, capacity 20 m^3/d.

2.1. Materials

The Cu-Ni alloys are commonly used in the heat exchanger tubes in MSF plants, in recovery and heat rejection sections. The materials designations are: Cu-Ni 90/10, Cu-Ni 70/30. The analyses for the composition of the coupons were carried out using optical emission spectrometer (OES). The composition of the alloys is shown in Table 1.

Three coupons of each material (Cu-Ni 90/10, Cu-Ni 70/30) were used in these experiments. The coupons size was 50 × 20 × 5 mm, surface grinding to 180 grit (by emery paper). The coupons were then rinsed with distillated water and cleaned with acetone before fixing in the vapor zone. The operational parameters of the plant were closely monitored, and any variations in the parameters were reported during operation. The weight loss coupon technique was used for corrosion rate measurements

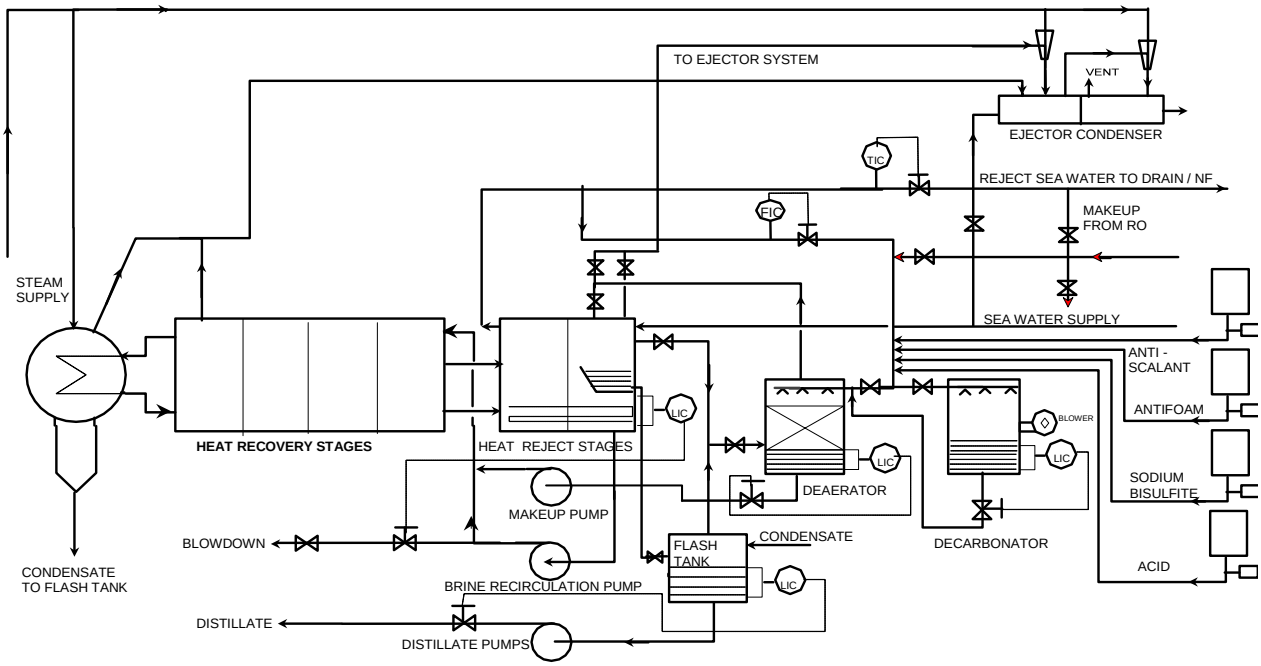

Fig. 3. Schematic diagram of the MSF pilot plant [15].

Table 1
Composition of alloys investigated in the studies

Element	90/10 Cu-Ni	70/30 Cu-Ni
Fe	1.4486	0.0054
Ni	8.7998	30.621
Mn	0.24126	0.6224
Cu	Balance	Balance

following ASTM standards for laboratory immersion corrosion testing of metals. (G31-72, re-approved 1-90) and conducting corrosion coupon test in plant equipment (G4-84).

2.2. Test conditions and duration

The test was carried out at four different top brine temperatures (TBT) namely 90°C, 100°C, 110°C and 119°C. These temperatures represent the different modes of operation of MSF plants where 90°C is for low additive dosed plants such as Al-Jubail phase II, while 100°C and 110°C for high temperature additive such as Yanbu plants and Jeddah phase III, and 119°C represents high temperature in MSF plants (acid treat plants) before the hard scale is formed at 121°C. In 119°C MSF pilot plant test, additive was used to control the scale formation.

The temperature difference in each stage is affected by the difference between the first (top brine temperature) and last stages and the number of the stages. The test duration was 480 h (20 d). This period is recommended for the plant test and is sufficient for the test in pilot plants [16,17]. The conditions in the MSF pilot plant stages during the different tests are shown in Table 2. The test coupons were exposed to chlorinated Gulf seawater taken from the intake at Al-Jubail MSF plants and fed to the MSF pilot plants. The composition of the Gulf seawater is given in Table 3.

After the completion of tests, the coupons were photographed, visually inspected and some of the coupons were further examined by SEM and EDX.

Table 3
Composition of Gulf seawater at Al-Jubail [19]

Constituents	Arabian Gulf Seawater, Al-Jubail
Cations (ppm)	
Sodium Na^+	13440
Potassium K^+	483
Calcium Ca^{2+}	508
Magnesium Mg^{2+}	1618
Copper Cu^{2+}	0.004
Iron Fe^{3+}	0.008
Strontium Sr^{2+}	1
Boron B^{3+}	3
Anions (ppm)	
Chloride Cl^-	24090
Sulfate SO_4^{2-}	3384
Bicarbonate HCO_3^-	130
Carbonate CO_3^{2-}	—
Bromide Br^-	83
Fluoride F^-	1
Silica SiO_2	0.09
Other parameters	
Conductivity, mS/cm	62800
pH	8.1
Dissolved oxygen, ppm	7
Carbon dioxide, ppm	2.1
Total suspended solids, ppm	20
Total dissolved solids, ppm	43800

2.3. Coupons location

The coupons were fixed in stage one (highest temperature), stage three (middle stage and medium temperature) in heat recovery section and stage five (last stage and lowest temperature) in heat reject section at the MSF pilot plant in a way to be above the demister and below the condenser tube. Additionally to the above in some tests there were two different arrangements of the position of the coupons: vertical where the vapor passes beside the coupon and horizontal where the vapor hit the face of the coupon were also carried out. Fig. 4 shows the arrangements used in the experiments.

Table 2
Conditions existing at the MSF pilot plant during the different tests [18]

Temperature	90°C		100°C		110°C		119°C	
Stages	Brine temp., °C	Vapor temp., °C	Brine temp., °C	Vapor temp., °C	Brine temp., °C	Vapor temp., °C	Brine temp., °C	Vapor temp., °C
Stage 1	90	81	100	89.4	110	98	119	104.8
Stage 3	73.5	64	78.1	68.73	86.8	73.8	94.2	80.1
Stage 5	45.25	38.7	48.75	41.7	52.2	43.6	56.9	47.8

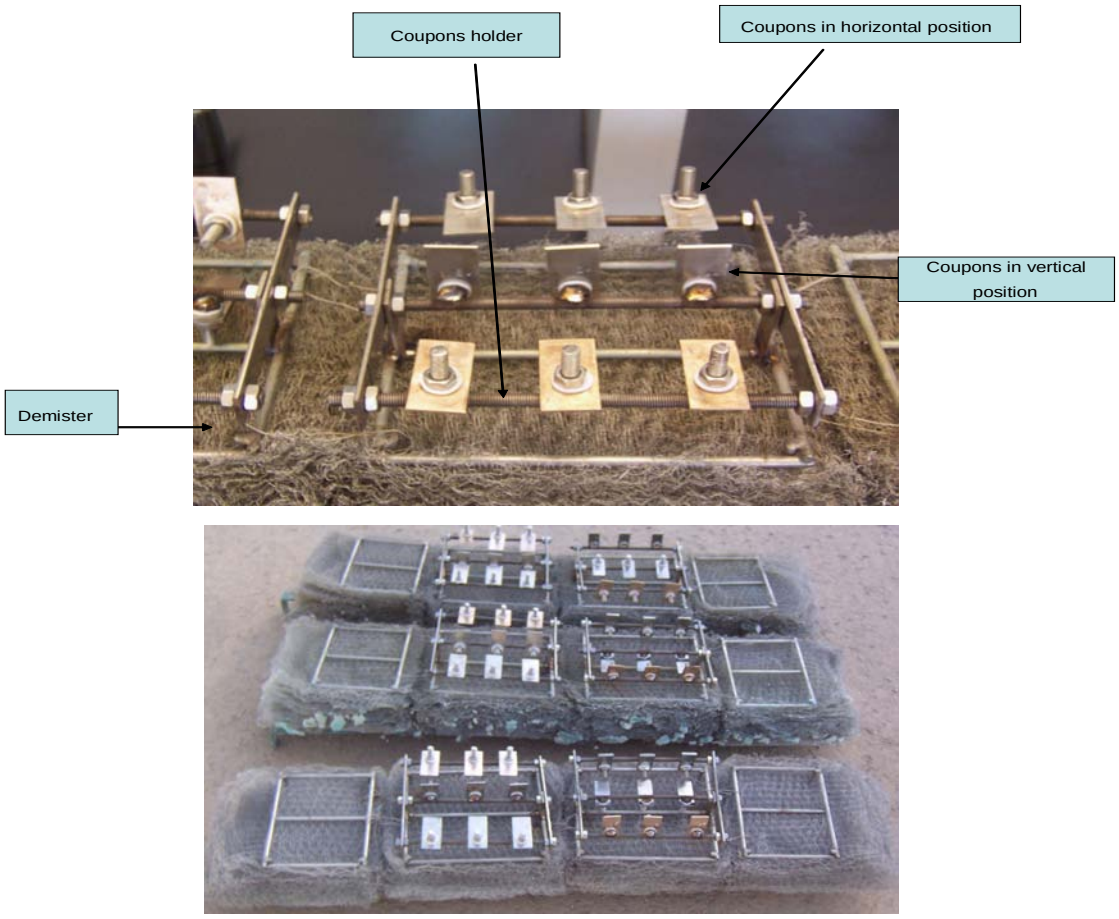

Fig. 4. Upper — the photograph shows the coupon arrangements in stages one, three and five; lower — coupons in the three stages before being placed in the MSF pilot plant.

3. Results

3.1. Tests at 90°C (TBT)

The first test in the MSF pilot plant was exposing the coupons to 90°C (TBT) at the first stage, third stage and fifth stage. At 90°C the MSF pilot plant is under atmospheric pressure. This simply means that the evaporator is under reduced pressure (vacuum) in the first stage and the remaining stages. This will eventually lead to air leakage to the unit. In this test the coupons were exposed in vertical position. Fig. 5 shows the appearance of test coupons immediately after the experiment completion and before removal from the holder in stage one of the MSF pilot plant. Fig. 6 shows the appearance of Cu-Ni coupons after the conclusion of the test for stage one, stage three and stage five and the corrosion rates for coupons at stage one, three and five are shown in Table 4.

3.2. Tests at 100°C (TBT)

Fig. 7 shows the appearance of coupons immediately after the test completion at 100oC (TBT) and before removal of the coupons from the holder in stage one. Fig. 8

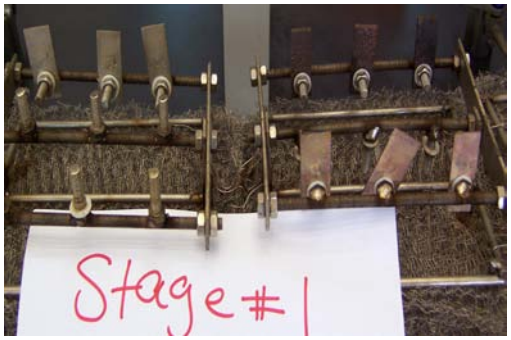

Fig. 5. Appearance of the Cu-Ni alloys at the end of the test at 90°C (TBT) at stage one.

shows a close look on the coupons individually in vertical and horizontal positions for stage one. Table 5 gives the corrosion rate for the coupons in stage one at 100°C (TBT) in the two positions (vertical and horizontal).

3.3. Tests at 110°C (TBT)

Fig. 9 shows the appearance of coupons immediately

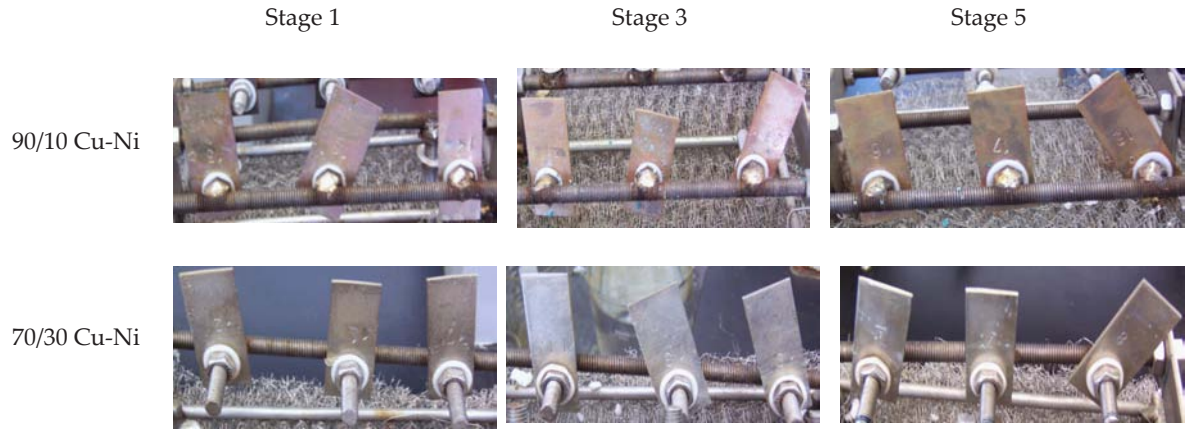

Fig. 6. Appearance of 90/10 Cu-Ni and 70/30 Cu-Ni after the conclusion of the test for stage one, stage three and stage five at 90°C (TBT) in the MSF pilot plant.

Table 4
Corrosion rate for the coupons at the end of test at 90°C (TBT) for stages one, three and five

Material	Corrosion rate (mpy)		
	Stage 1	Stage 3	Stage 5
Cu-Ni(90-10)	0.1886	0.2227	0.1530
Cu-Ni(70-30)	0.0533	0.0647	0.0369

Fig. 7. The photograph shows the appearance of coupons after the test completion at 100°C (TBT) at stage one.

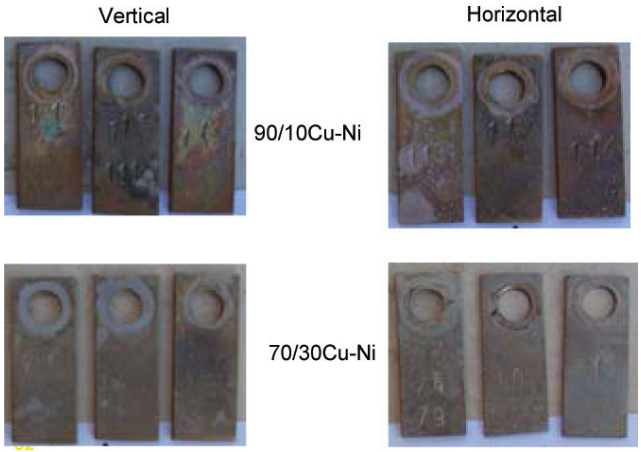

Fig. 8. Appearance of coupons in stage one in vertical and horizontal positions at temperature100°C (TBT).

after the test completion and before removal of the coupons from the holder in stage one. Fig. 10 shows a close look of the coupons individually. Table 6 provides corrosion rates at the end of the test at 110oC (TBT) for stage one, three and five in vertical and horizontal positions respectively. Figs. 11 and 12 show the SEM pictures and EDX spectra for the Cu-Ni (90/10 and 70/30) respectively after exposure to this temperature.

Table 5
Corrosion rates for Cu-Ni alloys at the end of the test at100°C (TBT) for stages one, three and five in vertical and horizontal positions respectively

Material	Corrosion rates (mpy) for stage one, three and five at 100°C (TBT)					
	Stage one		Stage three		Stage five	
	Vertical	Horizontal	Vertical	Horizontal	Vertical	Horizontal
Cu-Ni (90-10)	0.1265	0.0860	0.2464	0.2616	0.1477	0.0877
Cu-Ni (70-30)	0.1018	0.1404	0.0914	0.1009	0.0571	0.0484

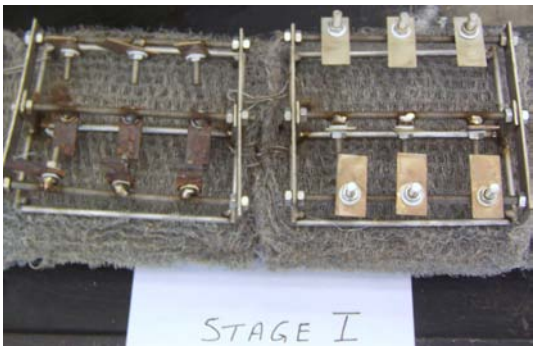

Fig. 9. Appearance of coupons immediately after the completion of the test at 110°C (TBT) at stage one.

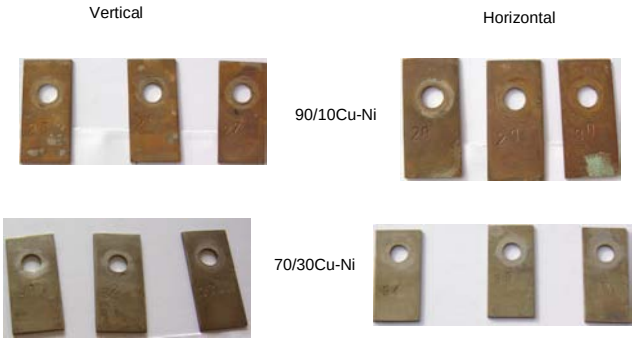

Fig. 10. Appearance of coupons in vertical and horizontal positions immediately after the completion of the test at 110°C (TBT) at stage one.

Table 6
Corrosion rates at the end of the test at 110°C (TBT) for stage one, three and five in vertical and horizontal positions respectively

Material	Corrosion rates (mpy) for stage one, three and five at 110oC (TBT)					
	Stage one		Stage three		Stage five	
	Vertical	Horizontal	Vertical	Horizontal	Vertical	Horizontal
Cu-Ni (90-10)	0.1880	0.1927	0.1193	0.1304	0.1823	0.1135
Cu-Ni (70-30)	0.1072	0.0951	0.0465	0.0707	0.0423	0.0485

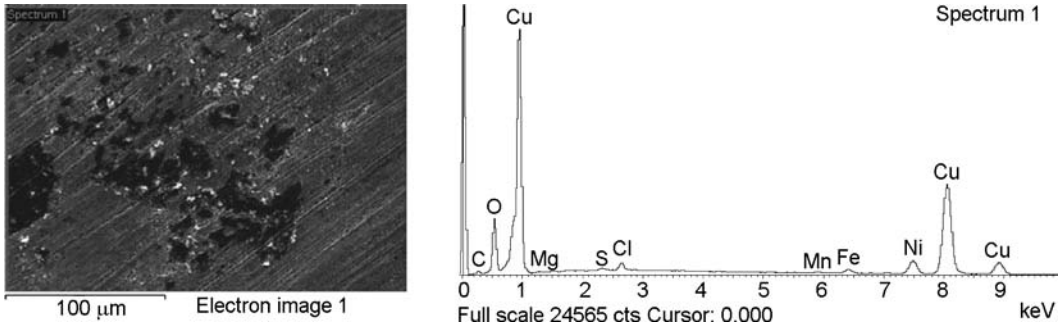

Fig. 11. (a) SEM picture; (b) EDX spectrum of the oxide scales for the 90/10 Cu-Ni coupons in stage one at 110°C (TBT).

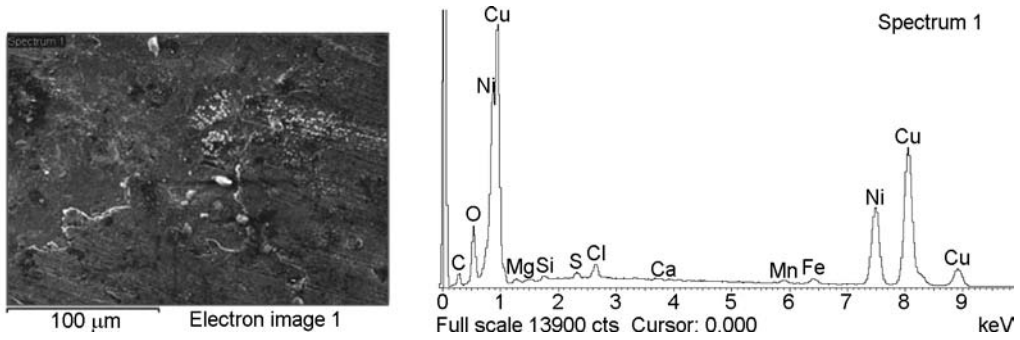

Fig. 12. (a) SEM picture; (b) EDX spectrum of the oxide scales for the 70/30 Cu-Ni coupons in stage one at 110°C (TBT).

3.4. Tests at 119°C (TBT)

Fig. 13 shows a close look of the appearance of coupons immediately after the test completion individually in stage one, three and five. The corrosion rates at these stages are shown in Table 7. Figs. 14 and 15 show the SEM picture and EDX profile for the Cu-Ni (90/10 and 70/30) respectively after exposure to this temperature.

Based on the results indicated in Table 7 the following points can be drawn:

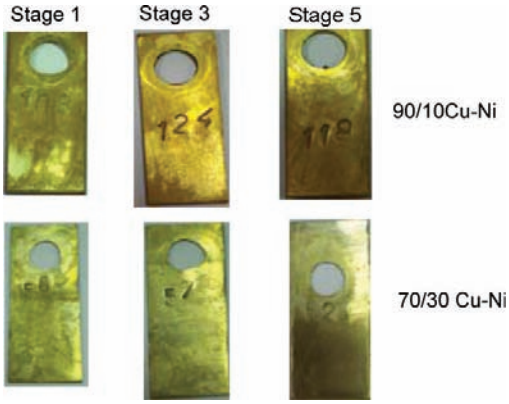

Fig. 13. Appearance of coupons immediately after the completion of the test at 119°C (TBT) at stage one, three and five.

Table 7
Corrosion rates for the coupons at the end of the test at 119°C (TBT) for stage one, three and five

Material	Corrosion rate (mpy)		
	Stage 1	Stage 3	Stage 5
Cu-Ni(90-10)	0.2568	0.1416	0.1147
Cu-Ni(70-30)	0.0491	0.0361	0.0320

1 The corrosion rate in stage one (which is not under atmospheric pressure so the air leakage is minimum) for the coupons Cu-Ni 90/10 and Cu-Ni 70/30 is higher than in the other two stages. This indicates that temperature plays a role, and not oxygen.
2 The corrosion rate of Cu-Ni 70/30 is lower than that of Cu-Ni 90/10 which is in agreement with the other test and with published papers [11,12].
3 By comparing the results obtained at 119°C (TBT) (highest temperature) with the test carried out at 90°C (TBT) (lowest temperature), it could be observed that for 90/10 Cu-Ni alloys the corrosion rate at 90°C is higher in stage three and five than at 119°C. For Cu-Ni 70/30 it is slightly higher in all stages at 90°C compared with 119°C.

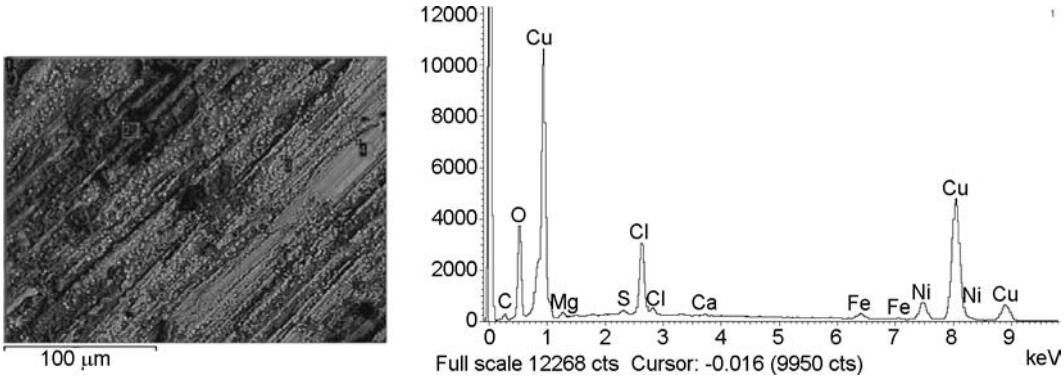

Fig. 14. (a) SEM picture; (b) EDX spectrum of the oxide scales for the 90/10 Cu-Ni coupons in stage one at 119°C (TBT).

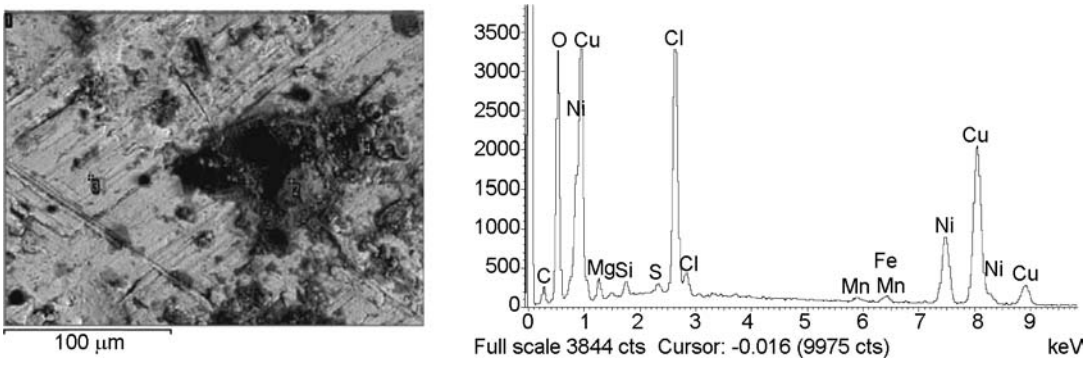

Fig. 15. (a) SEM picture; (b) EDX spectrum of the oxide scales for the 70/30 Cu-Ni coupons in stage one at 119C (TBT).

This shows that the corrosion rate increases due to air leakage (strong factor) and not due to the increase of temperature.

3.4. Stages vs. temperature

Fig. 16 shows the relation of vapor zone temperature with the corrosion rate for the coupons at stage one, three and five in the MSF pilot plant at the four temperatures. It is obvious from this figure that there is irregular behavior of temperature with corrosion of copper nickel alloys.

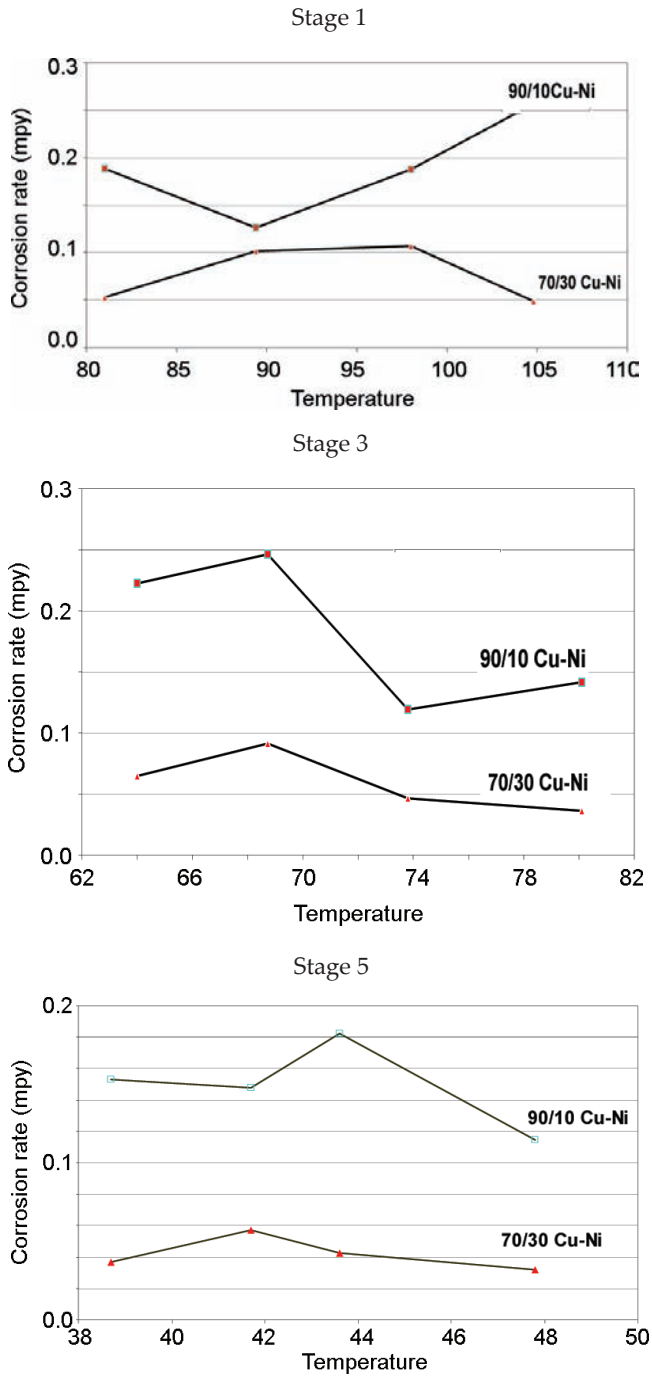

Fig. 16. Corrosion rate for coupons at stage one, three and five in MSF pilot plant at different vapor zone temperatures.

4. Discussion

The main aim of these studies is to determine the corrosion performance of the materials of heat exchanger tubes used in MSF evaporators, namely Cu-Ni 90/10 and Cu-Ni 70/30 alloys, by conducting experiments in the MSF pilot plant at four different top brine temperatures.

The VSC studies in the MSF pilot plant evaporator carried out under reduced pressure at 90°C (TBT) in stage one shows high corrosion rate values (in mpy): 90/10 Cu-Ni — 0.19 and 70/30 Cu-Ni — 0.05, which is profoundly low. The corrosion rates of the alloy in stage three are: 90/10 Cu-Ni — 0.22 and 70/30 Cu-Ni —0.065, which is slightly higher than in stage one. In stage five the rates are: 90/10 Cu-Ni — 0.015 and 70/30 Cu-Ni — 0.037, which is lower than stage three and one.

Although stage one at 90°C (TBT) has the highest temperature compared to stage three and stage five and where it will be expected that NCG will be more in this stage compared to other stages due to thermal decomposition of bicarbonate, the corrosion rate for Cu-Ni alloys at stage one is higher than at stage five for both compositions but less than at stage three. This could be attributed to the role of combined effect of temperature and air leakage at stage three where the air leakage is expected to be more in this stage compared with stage one in addition to that cascading of NCG which accumulate in this stage. It is indicates their is an interaction between the effects of temperature, oxygen, carbon dioxide and the air leakage (oxygen) is the strong factor. This finding is in agreement with the results of the test carried out at Al Khafji plant [20] where the authors attributed it to the combined effect of temperature, air leakage and cascading of NCG at the middle stages. In general, Cu-Ni alloys have relatively low corrosion rates. At 90°C, the corrosion rates of 90/10 Cu-Ni are higher than those of 70/30 Cu-Ni alloys which is an agreement with the available literature [11,12].

At 100°C (TBT) horizontal and vertical coupons were used. In stage one and stage five, Cu-Ni, 90/10 has higher corrosion rate in the vertical position compared with the horizontal one. For Cu-Ni, 70/30 the opposite behavior is observed except for stage five. The higher corrosion rates in horizontal position have been attributed to the exposure of the vapor phase to a much higher surface area. A glance on the corrosion rate values of the coupons at the vertical and horizontal positions points out that the differences are very small. Whilst the corrosion rates in stage three are higher in the horizontal position, in stage five, higher corrosion rates in vertical position. At 100°C (TBT), in stage three the corrosion rates of 90/10 Cu-Ni and 70/30 Cu-Ni are similar at both positions.

The results of 110°C (TBT) show that in stage one, the

corrosion rate of 90/10 Cu-Ni in the horizontal positions is higher than in the vertical position, for 70/30 Cu-Ni, the behavior is opposite although the difference in corrosion rates is marginal. In stage three, the corrosion rates of alloys at 110°C, in vertical position are invariably lower than for horizontally positioned alloys. In stage five, 110°C, the corrosion rates in horizontal position for 90/10 Cu-Ni are lower than in vertical positions. For 70/30 Cu-Ni, the corrosion rates of vertical and horizontal positions are very low and have almost the same value.

In 119°C (TBT) test, stage one, the corrosion rates for 90/10 Cu-Ni and 70/30 Cu-Ni are 0.25, and 0.049 mpy, respectively. In stage three the corrosion rates of the two alloys are lower than those in stage one. The corrosion rates of 90/10 Cu-Ni are about one order of magnitude higher than 70/30 Cu-Ni. At 119°C, stage five, the corrosion rates of cupronickel alloys are lower than in stages one and three.

Considering the corrosion behavior of the alloys at different stages of the MSF pilot plant in vertical position, in stage one, for 90/10 Cu-Ni, the highest corrosion rate was observed at 119°C, the corrosion rates at 90°C and 110°C are equal and for 70/30 Cu-Ni, the corrosion rates are highest at 100°C and 110°C and lowest at 119°C. In general, the corrosion rates of 90/10 Cu-Ni are much higher than those of 70/30 Cu-Ni showing the latter as better corrosion resistant.

In stage three, for 90/10 Cu-Ni, the highest corrosion rate is noted at 100°C and the lowest at 110°C. For 70/30 Cu-Ni, the highest corrosion rate is noted at 100°C and the lowest at 119°C. In general, in stage three, the lowest corrosion rates for the alloys are observed at 110°C and 119°C.

In stage five, for 90/10 Cu-Ni alloys, corrosion rates are highest at 110°C and lowest at 119°C. For 70/30 Cu-Ni, corrosion rates are highest at 100°C and lowest at 119°C.

Summing up the corrosion performance of cupronickel 90/10 and 70/30 alloys in vertical and horizontal positions at 90°C, 100°C, 110°C and 119°C vis-à-vis stages one, three and five at which studies were carried out in MSF pilot plant. At 90°C, each of the two alloys has the highest corrosion rate in stage three. At 100°C, the corrosion rates of 90/10 Cu-Ni are highest in stage three and those of 70/30 Cu-Ni in stage one. This behavior in vertical and horizontal positions at 110°C, 90/10 Cu-Ni has the same corrosion rate of 0.19 mpy in stage one and five. For 70/30 Cu-Ni, the highest corrosion rate is noted in stage one for both vertical and horizontal positions. At 119°C, the highest corrosion rates are observed in stage one. Fig. 16 shows that there is irregular behavior of corrosion rates of Cu-Ni with respect to temperatures which is in agreement with literature [21].

The morphological studies were carried out on oxide scales formed during VSC at different temperatures (90°C, 100°C, 110°C and 119°C) and stages (one, three and five) for cupronickel (90/10 and 70/30). In general, horizontally positioned alloy formed thicker scales. The oxide scales on cupronickel (90/10 and 70/30 Cu-Ni) at 90°C have similar morphologies at all the three stages, 90/10 Cu-Ni forms dark to light brown cupric oxide deposits, 70/30 Cu-Ni oxide scales are light and have invariably green products inclusion presumably cupric oxide along with copper basic carbonate.

At 100°C, 90/10 cupronickel coupons show brown CuO scales. In 70/30 Cu-Ni, green products which are presumably of Ni oxide and/or copper basic carbonate appeared along with brown cupric oxide.

At 110°C, in stage one, in 90/10 Cu-Ni alloys, the scales are brownish along with greenish products at some locations. In 70/30 Cu-Ni, the scales are relatively thin. The SEM and EDX studies on the corrosion products formed on cupronickel alloys after exposure to vapor side show the presence of copper oxide in predominant concentration. In case of 90/10 Cu-Ni alloy, Ni is present in an extremely low concentration (Fig. 11b) but in 70/30 Cu-Ni alloy, NiO is present in a much higher concentration (Fig. 12b). At 119°C, 90/10 Cu-Ni alloy shows layered scales containing copper oxide with high concentration of Cl perhaps in the form of Mg chloride. There is no perceptible presence of Ni. The scales formed on 70/30 Cu-Ni alloy at 119°C are generally uniform but disrupted at some locations as indicated by the SEM picture. The morphology of the scales indicates the presence of NiO and CuO with inclusions of chloride of Ca and Mg. The EDX profile shows strong peaks of Ni, Cu and O and moderately strong peak of Cl.

For the disruption of the protective film on the copper alloys two mechanisms have been suggested [22] — one relates the disruption of the protective film by the external atmosphere which causes local attack due to the presence of aggressive gases such as CO_2 ,O_2 etc., the second cause of the disruption of the protective film is the condensation/evaporation of water vapor droplets.

Apart from water vapor which is always present, the gases evolved from flashing brine in the MSF process consist mainly of CO_2, air (oxygen and nitrogen). In acid treated plant, most of CO_2 is removed by decarbonator before the seawater feed to the plant while in additive-dosed plant, the CO_2 produced due to the thermal decomposition of bicarbonate and CO_3^{2-} combines with water vapor to acquire acidic character which lowers the pH to acidic value and this affects the protective film. Although a low pH will not itself cause corrosion of copper alloys, it can damage protective films and allow the oxygen present to cause corrosion. It is suggested that this acidic character will cause failure of 90/10 Cu-Ni condenser tubes in MSF plants as reported by Asrar [23]. The final report on Dow Freeport program does state that unless CO_2 is effectively removed from the feed to the heat recovery section it will form low pH carbonic acid in the vapor zone and lead to increased vapor side corrosion (VSC). El-Dahshan et al. [24] suggested two mechanisms for VSC depending on

the nature of the environment — either acidic or alkaline media. Shames El Din et al. [1] believed that it would be over simplified to attribute failure of copper alloys tube in terms of acidity created as a result of CO_2 dissolution. This is because both copper and its alloy are above hydrogen in the electro-chemical series, hence they cannot displace H+ ions from acid solution. Thus they concluded that the presence of both O_2 and CO_2 in the atmosphere of the evaporator is essential for active dissolution of condenser tubes. It is to be noted that reduction of O_2 alone does not account for VSC of the condenser tube. In natural vapor O_2 reduction favors the formation of adherent, protecting copper oxide on the tube surface.

In the present case, in the mechanism of VSC of Cu-Ni alloys there is involvement of both CO_2 ,O_2 and also carry over Cl^-. If the oxide scales are disrupted at any stage of the exposure, the local action is predominated. In the initial stages, copper oxide scales are formed following a reaction sequence involving anodic and cathodic reactions presented by Shames El Din et al. [1].

Corrosion products formed during oxidation and with carbonic acid may react further with Cl^- to give complex species such as $CuCl_2.3Cu(OH)_2$ or $CuCl_2.3Cu(OH)_3Cl$ building up multilayered thick scales.

Due to inherent resistance of Ni, in most cases, 70/30 Cu-Ni alloys showed lower CO_2 induced VSC than 90/10 Cu-Ni alloys.

5. Conclusions

1 90/10 Cu-Ni has higher corrosion rates than 70/30 Cu-Ni in the test carried out at 90,100, 110 and 119°C in the MSF pilot plant. This is in agreement with the findings in literature.
2 For 90/10 Cu-Ni alloys the corrosion rates at 90°C are higher than at 119°C in stage three and five. For Cu-Ni 70/30 it is slightly higher in all stages at 90°C compared to 119°C. This indicates that air leakage due to vacuum is a strong factor, and not temperature.
3 The corrosion rates for Cu-Ni alloys in the vertical orientation are higher than in horizontal orientation in some tests. This is due to a short period of the test (20 days).
4. In stage one the corrosion rates at 119°C in the MSF pilot plant are the highest and the lowest at 100°C. For stage three the highest rates are observed at 100°C and for stage five — at 90°C. This indicates that there are interactions of temperature, air leakage and NCG formed during the evaporation process.

References

[1] A.M. Shams El Din and R.A. Mohammed, Contribution to the problem of vapour-side corrosion of copper-nickel tubes in MSF distillers, Desalination, 115 (1998) 135–144.
[2] J. Oldfield and B. Todd, Vapor side corrosion in MSF plants, Desalination, 66 (1987) 171–184.
[3] A.H. Tuthill, B. Todd and J. Oldfield, Experience with copper alloy tubing, waterboxes and piping in MSF desalination plants, Proc. IDA World Congress, Madrid, Spain October 6–9, 1997.
[4] A.U. Malik and P.C. Mayan Kutty, Corrosion and Material Selection in Desalination Plants, Research Activities and Studies, SWCC Publication No. 3, 1992.
[5] J. Oldfield. and B. Todd, Corrosion consideration in selecting materials for flash chambers, Desalination, 31 (1979) 365–383.
[6] A. Al-Arifi, Mechanistic studies of vapor side corrosion in MSF desalination plants, PhD thesis submitted to University of Manchester, Institute of Science and Technology, King Saud University, 2009.
[7] I.S. Al-Mutaz, M.A. Alodan, F. Abudaleem and A. Al-Arifi, Experimental investigation of vapor side corrosion in multistage flash desalination plants, Proc. IDA World Congress, Maspalomas, Spain, 2007.
[8] I.S. Al-Mutaz, M.A. Alodan, F. Abudaleem and A. Al-Arifi, Review of vapor side corrosion in multistage flash desalination plants, Proc. IDA World Congress, Bahamas, 2003.
[9] A.M. Shams El Din, R.A. Mohammed and H.H. Haggag, Electrochemical simulation of vapour-side corrosion of Cu-Ni condenser tubes in MSF distillers, Br. Corrosion J., 35 (2000) 237–240.
[10] T. Hodgkiess and D. Mantzavinos, Corrosion of copper–nickel alloys in pure water, Desalination, 126 (1999) 129–137.
[11] K.Z. Al-Subaie and T. Hodgkiess, Corrosion of copper–nickel alloys in simulated vapor-side environments, Desalination, 158 (2003) 43–50.
[12] M.A. Al-Thubaiti, T. Hodgkiess and S.Y.K. Ho, Environmental influence on vapor-side corrosion of copper–nickel alloys, Desalination, 183 (2005) 711–718.
[13] K. Abouswa, F. El Shawesh, O. Elrage and A. Elhood, Corrosion investigation of Cu-Ni tube desalination plant, Desalination, 205 (2007) 140–146.
[14] E.E. El Sayed, A. Al-Odwani, M. Safer and M. Al-Tabtabaei, MSF test unit for corrosion studies: testing of six different alloys, ARWATEX, Riyadh, Saudi Arabia, April 2008.
[15] O. Hamed, Prospects of development of thermal desalination processes, Proc. SWCC 5th Acquired Experience Symposium, Al-Khobar, 5–7 January 2008.
[16] M.G. Fontana and N.D. Greene, Corrosion Engineering. McGraw-Hill, New York, 1967.
[17] F.P. Ijesseling, General guideline for corrosion testing of materials for marine applications, Br. Corrosion J., 24(1) (1989) 55–77.
[18] MSF pilot plant operation data sheet.
[19] SWCC Al-Jubail Plant Laboratory Analysis.
[20] N. Asrar, A.U. Malik, S. Ahmed, M. Al-Khalidi and K. Al-Moaili, Corrosion monitoring of SWCC plants. 1: Vapor side corrosion monitoring in Al-Khafji desalination, Research Activates and Studies, SWCC Publication, 7 (1997) 287–331.
[21] M.S. Parizi, A. Aladjem and J.E. Castle, Behaviour of 90-10 cupronickel in seawater, Intern. Materials Rev., 33(4) (1988) 169–200.
[22] E.A. Al-Sum, S. Aziz, A. Al Radif, M. Samir and O. Helkal, Vapour-side corrosion of copper based condenser tubes of the MSF desalination plants of Abu Dhabi, Desalination, 97 (1994) 109–119.
[23] N. Asrar, A.U. Malik, S. Ahmed, A. Al-Sheikh, F. Al-Ghamdi and M.A. Al-Thobiety, Early failure of cupro-nickel condenser tubes in thermal desalination plant, Desalination, 116 (1998) 135–144.
[24] M.E. El-Dahshan and B. Bin Ashoor, Case studies of corrosion of distillers tubing materials, Proc. IDA World Congress, Bahamas, 2003.